Bioelectrochemistry as a tool for the study of aromatization of steroids by human aromatase

UNIVERSITÀ DEGLI STUDI DI TORINO

Bioelectrochemistry as a tool for the study of aromatization of steroids by human aromatase

Giovanna Di Nardo,[§] Silvia Castrignanò,[§] Sheila J. Sadeghi, Roberta Baravalle, and Gianfranco Gilardi*

Department of Life Sciences and Systems Biology, University of Torino, Via Accademia Albertina 13, Torino, Italy

*Corresponding to**:** Prof. Gianfranco Gilardi, Department of Life Sciences and Systems Biology, University of Torino, via Accademia Albertina 12, 10123, Torino, Italy, Tel: +390116704593; Fax: +390116704643; E-mail: gianfranco.gilardi@unito.it

[§]GD and SC equally contributed to this work.

Abstract

Bioelectrochemical conversion of androgens into estrogens was achieved using human aromatase immobilized on glassy carbon electrodes. According to substrate concentration used in the electrochemical cell, it was possible to accumulate the intermediates or to proceed toward the formation of the final estrogen product confirming the distributive nature of catalytic reaction. Furthermore, the catalytic rates showed that the first step of reaction is the limiting one.
The results demonstrate that bioelectrochemistry can be employed for understanding complex enzymatic reactions, such as aromatization of steroids.

Keywords

Aromatase, Protein immobilization, Cytochrome P450, Estrogens

1. INTRODUCTION

Aromatase is a cytochrome P450 that catalyses a three steps reaction leading to the conversion of androgens into estrogens [1-3]. Since this enzyme is overexpressed in estrogen-dependent tumors, it is an important pharmacological target and aromatase inhibitors are currently used to treat breast cancer in post-menopausal women [4]. Furthermore, aromatase plays a role in the development of neurodegenerative disorders such as Alzheimer's disease [5].
Aromatase reaction proceeds through the formation of two stable intermediates (19-hydroxy- and 19-oxo-) deriving from 2 consecutive hydroxylation reactions at C19. In the third and last step, the removal of C19 as formic acid and the abstraction of protons from the A-ring cause the aromatization of the steroid molecule with the generation of the final estrogen product (Scheme 1) [6-8].
The conversion of androgen substrates into estrogen products is mediated by cytochrome P450 reductase (CPR) and requires 6 electrons donated from 3 NADPH molecules [9]. Furthermore, pulse-chase experiments suggest that the enzyme is distributive rather than processive [10]. This means that intermediates of the reactions are free to be accepted in, and can dissociate from, the protein active site according to their affinities for the enzyme.
Here, recombinant human aromatase (rArom), sharing the same structural features as full-length enzyme [11,12], was immobilised on glassy carbon electrodes. Direct electrochemistry and bioelectrocatalysis experiments were performed for the study of its catalytic reaction and comparison to the data for the protein in solution.

2. MATERIAL AND METHODS

2.1 Aromatase preparation

Recombinant aromatase (rArom) was purified as described before [13]. For the preparation of rArom in complex with substrate or intermediates, saturating amounts of androstenedione (AD, 10 μM), or 19-hydroxyandrostenedione (19-OHAD, 150 μM) or 19-oxoandrostendione (19-OXOAD, 150 μM) were added in the purification buffers.

2.2 Immobilization procedure

Substrate-free and rArom in complex with AD, 19-OHAD and 19-OXOAD were immobilized on poly-diallyldimethylammonium chloride (PDDA) [14] modified glassy carbon (GC) electrodes (area of 0.07 cm^2 - BASi) [15-19]. A 1:1 (5 μl + 5 μl) mixture of pure PDDA and protein solution (85 μM) was cast onto clean GC electrodes and allowed to set overnight at 4 °C.

2.3 Electrochemical measurements

Electrochemical experiments were performed at room temperature in 50 mM phosphate buffer pH 7.4, containing 100 mM KCl as supporting electrolyte, using an Autolab PGSTAT12 potentiostat (Ecochemie). A cell equipped with a platinum counter electrode, an Ag/AgCl (3 M NaCl) reference electrode and a GC working electrode (BASi) was used.
The detectability of rArom on PDDA electrodes was investigated using cyclic voltammetry (CV) by scanning the potential between 200 and -600 mV at increasing scan rate values (from 20 to 120 mV sec^{-1}). CV experiments were performed in a glove box to ensure anaerobic conditions.
Redox properties of rArom were also investigated using square wave voltammetry (SWV) between 0 and -600 mV (step potential: 5 mV; amplitude: 50 mV; scan frequency: 50 Hz).
Electrocatalysis was performed using chronoamperometry with an applied potential of -600 mV for 30 min. To minimize mass transport influence, rotating disk electrodes were used on a BASi RDE-2 rotator system. Chronoamperometry was applied on freshly prepared electrodes and the product obtained after 30 minutes was immediately quantified by high performance liquid chromatography (HPLC).

2.4 HPLC analysis of the reaction products

Identification and quantification of electrocatalysis products were achieved by HPLC coupled with a diode array UV-vis detector equipped with an Eclipse Plus-C18 column (Agilent Technologies). The mobile phase was a mixture of water and acetonitrile. Standards of AD, 19-OHAD, 19-OXOAD and estrone (Sigma Aldrich, purity ≥ 98%) were used to establish retention times, UV-vis spectra and to construct calibration curves by injecting known amounts of each compound. Mixtures of standards were also injected to exclude potential interferences between the different steroids. AD, 19-OHAD and 19-OXOAD were detected and quantified at 237 nm, whereas estrone was followed at 280 nm.

3. Results and discussion

3.1 Direct electrochemistry of human aromatase

Direct electrochemistry of rArom (55 kDa) immobilized on PDDA-modified glassy carbon electrodes both in the AD-free and -bound form was performed by CV and SWV (Figure 1) in anaerobic conditions (< 10 ppm oxygen). In both cases, a single redox couple corresponding to heme $Fe^{III/II}$ transition was detected. Reduction potentials measured from SWV were -284 mV and -247 mV versus Ag/AgCl for substrate-free and –bound rArom, respectively (Table 1), consistent with published data on direct electrochemistry of CYP enzymes [16,20-23]. CV applied to protein previously denatured by 6 M guanidinium hydrochloride resulted in a midpoint potential of -42 mV (versus Ag/AgCl). Using CV, for both rArom immobilized in presence and absence of the substrate AD, a linear dependency was found between peak currents and scan rate (Figure 1C). This is characteristic of thin film confined electroactive species that are not under diffusion control [24]. Moreover, the calculated surface coverage of rArom was 2.9 ± 0.2 pmol cm^{-2}.

Reduction potentials of rArom in complex with the intermediates 19-OHAD and 19-OXOAD are similar to those obtained for AD complex and positively shifted with respect to the substrate-free enzyme (Table 1). These results are consistent with the substrate-induced positive shift of reduction potential essential for the electron transfer from cytochrome P450-reductase (CPR) to the catalytic heme in cytochromes P450 [25,26].

3.2 Electrocatalysis experiments

Experiments were initially performed with immobilized substrate-free rArom. In presence of saturating amounts of AD (up to 100 μM) no reaction products were detected by HPLC analysis.

On the other hand, when rArom already in complex with AD was immobilized on the electrode surface, the product of the first step of the reaction, 19-OHAD (0.15 ± 0.05 μM), was detected (Figure 1). This result suggests that the immobilization process affects the flexibility of the protein, preventing substrate binding. It was shown that substrate-free human aromatase has a higher degree of flexibility compared to substrate-bound enzyme, necessary for accommodating the substrate as well as inhibitors [13,27]. Such a flexibility is reduced when the substrate is present [11-13,28].

An active enzyme was nevertheless obtained by this immobilization process and the first intermediate (19-OHAD) observed. This result suggests that the immobilized enzyme can either accept only 2 electrons or that AD amount is too high to allow the progression to the next reaction step. Indeed, the catalytic parameters for AD substrate and the 2 intermediates 19-OHAD and 19-OXOAD demonstrate that the enzyme has a 3 orders of magnitude higher affinity for AD than for the two intermediates [10]. Therefore, in excess of AD the enzyme prefers to accept AD and to form 19-OHAD, rather than to perform the second and the third steps of reaction leading to 19-OXOAD and estrone, respectively.

Taking into account these considerations, with the aim to test if the immobilized enzyme acts similarly as in solution, the concentration of AD was decreased to non-saturating concentrations (1 μM) [29] before immobilization to see if 19-OXOAD can be generated. Under these new conditions, 0.11 ± 0.03 μM of 19-OXOAD (Figure 1C) and small amounts of 19-OH (below the quantification limit) were detected. This result shows that the immobilized enzyme is able to proceed toward the second reaction step forming

19-OXOAD. When further lowering the AD concentration (less than 1 μM), no detectable intermediates or estrone were observed due to the detection limits of HPLC diode array.
The absence of the final product of aromatization, estrone, led us to check if it is also possible to bioelectrochemically drive the last aromatization reaction. Electrocatalysis was carried out using rArom in complex with the intermediates 19-OHAD (150 μM) and 19-OXOAD (150 μM) (Scheme 1). In the first case, electrocatalysis led to the formation of 19-OXOAD (0.31 ± 0.01 μM) and estrone (0.81 ± 0.08 μM). When 19-OXO is used, 1.69 ± 0.17 μM of estrone is observed (Figure 1D). This result shows that immobilized aromatase is able to catalyze also the final aromatization step. Moreover, it has been shown that the enzyme has a similar K_M for 19-OHAD and 19-OXOAD [10], resulting in the progression of the reaction toward the formation of the two consecutive products, 19-OXO and estrone, respectively. The data are again consistent with the distributive nature of the catalytic process.
Under our experimental conditions, a lower concentration of product is detected within the first step (from AD to 19-OHAD) compared to the third one (from 19-OXOAD to estrone). It is known that during the catalytic cycle of cytochromes P450, electrons can be wasted in uncoupling reactions. Our results support the view that rate and uncoupling level are different in the three reaction steps of human aromatase, with the last one being faster and more coupled. This is in line with recent studies on aromatase in solution [10] and incorporated into nanodiscs [30] where the rate of the last step of reaction as well as the coupling efficiency were shown to be higher compared to the first two.
Table 2 shows the summary of the amount of product obtained using AD, 19-OHAD and 19-OXOAD as starting substrates. The amount of product formed in the first step of reaction is one order of magnitude lower than the last step and therefore, when considering the overall three steps reaction, the limiting step is the first one. These results are in line with the data published before with the enzyme in solution [10].

4. CONCLUSIONS

Our data demonstrate that aromatase is active on the electrode surface. It is possible to bioelectrochemically obtain two out of three consecutive products by the same immobilized enzyme only by altering the equilibrium between the initial substrate and the intermediates (Scheme 1), providing the electrochemical evidence of the distributive nature of the three step reaction. Furthermore, the immobilised protein shows different product amounts for the first and third steps, suggesting that the conversion of androstenedione substrate into the first intermediate 19-OHAD is the limiting step for the whole reaction.

ACKNOWLEDGEMENTS

This work was supported by FIRB (project RBFR12FI27_004) and Progetto Ateneo 2012 (Sadeghi). Authors thank Prof. J. C. Hackett (VCU Massey Cancer Center) for the gift of 19-oxoandrostenedione.

References

[1] E.A. Thompson, P.K. Siiteri, The involvement of human placental microsomal cytochrome P-450 in aromatization, J. Biol. Chem. 249 (1974) 5373-5378.

[2] E.A. Thompson, P.K. Siiteri, Utilization of oxygen and reduced nicotinamide adenine dinucleotide phosphate by human placental microsomes during aromatization of androstenedione, J. Biol. Chem. 249 (1974) 5364-5372.

[3] E.R. Simpson, M.S. Mahendroo, G.D. Means, M.W. Kilgore, M.M. Hinshelwood, S. Graham-Lorence, B. Amarneh, Y. Ito, C.R. Fisher, M.D. Michael, C.R. Mendelson, S.E. Bulun, Aromatase cytochrome P450, the enzyme responsible for estrogen biosynthesis, Endocr. Rev. 15 (1994) 342-355.

[4] R.J. Santen, H. Brodie, E.R. Simpson, P.K. Siiteri, A. Brodie, History of aromatase: saga of an important biological mediator and therapeutic target, Endocr. Rev. 30 (2009) 343-375.

[5] M. Hiltunen, S. Iivonen, H. Soininen, Aromatase enzyme and Alzheimer's disease.Minerva Endocrinol. 31 (2006) 61-73.

[6] K. Sen, J.C. Hackett, Coupled electron transfer and proton hopping in the final step of CYP19-catalyzed androgen aromatization, Biochemistry 51 (2012) 3039-3049.

[7] P.J. Mak, A. Luthra, S.G. Sligar, J.R. Kincaid, Resonance Raman spectroscopy of the oxygenated intermediates of human CYP19A1 implicates a compound i intermediate in the final lyase step, J. Am. Chem. Soc., 136 (2014) 4825-4828.

[8] G. Di Nardo, G. Gilardi, Human aromatase: perspectives in biochemistry and biotechnology, Biotechnol. Appl. Biochem. 60 (2013) 92-101.

[9] A.Y. Lu, K.W. Junk, M.J. Coon, Resolution of the cytochrome P-450-containing x-hydroxylation system of liver microsomes into three components, J. Biol. Chem. 244 (1969) 3714-3721.

[10] C.D. Sohl, F.P. Guengerich, Kinetic analysis of the three-step steroid aromatase reaction of human cytochrome P450 19A1, J. Biol. Chem. 285 (2010) 17734-17743.

[11] D. Ghosh, J. Griswold, M. Erman, W. Pangborn, Structural basis for androgen specificity and oestrogen synthesis in human aromatase, Nature 457 (2009) 219-223.

[12] J. Lo, G. Di Nardo, J. Griswold, C. Egbuta, W. Jiang, G. Gilardi, D. Ghosh, Structural basis for the functional roles of critical residues in human cytochrome p450 aromatase, Biochemistry 52 (2013) 5821-5829.

[13] G. Di Nardo, M. Breitner, S.J. Sadeghi, S. Castrignanò, G. Mei, A. Di Venere, E. Nicolai, P. Allegra, G. Gilardi, Dynamics and flexibility of human aromatase probed by FTIR and time resolved fluorescence spectroscopy, PLoS One 8 (2013) e82118.

[14] S. Krishnan, J.F. Rusling, Thin film voltammetry of metabolic enzymes in rat liver microsomes, Electrochem. Commun. 9 (2007) 2359-2363.

[15] A. Fantuzzi, Y.T. Meharenna, P.B. Briscoe, C. Sassone, B. Borgia, G. Gilardi, Improving catalytic properties of P450 BM3 haem domain electrodes by molecular Lego, Chem. Commun. (Camb.) 12 (2006) 1289-1291.

[16] V.R. Dodhia, C. Sassone, A. Fantuzzi, G. Di Nardo, S. J. Sadeghi, G. Gilardi, Modulating the coupling efficiency of human cytochrome P450 CYP3A4 at electrode surfaces through protein engineering, Electrochem. Commun. 10 (2008) 1744-1747.

[17] S.J. Sadeghi, S. Ferrero, G. Di Nardo, G. Gilardi Drug-drug interactions and cooperative effects detected in electrochemically driven human cytochrome P450 3A4, Bioelectrochemistry 86 (2012) 87-91.

[18] F. Rua, S.J. Sadeghi, S. Castrignanò, G. Di Nardo, G. Gilardi, Engineering Macaca fascicularis cytochrome P450 2C20 to reduce animal testing for new drugs, J. Inorg. Biochem. 117 (2012) 277-284.

[19] S. Castrignanò, A. Ortolani, S.J. Sadeghi, G. Di Nardo, P. Allegra, G. Gilardi, Electrochemical detection of human cytochrome P450 2A6 inhibition: a step toward reducing dependence on smoking, Anal. Chem. 86 (2014) 2760-2766.

[20] M.J. Honeychurch, H.A.O. Hill, L.L. Wong, The thermodynamics and kinetics of electron transfer in the cytochrome P450cam enzyme system, FEBS Letts. 451 (1999) 351-353.
[21] A. Fantuzzi, M. Fairhead, G. Gilardi, Direct electrochemistry of immobilized human cytochrome P450 2E1, J. Am. Chem. Soc. 126 (2004) 5040-5041.
[22] H. Colas, K.M. Ewen, F. Hannemann, N. Bistolas, U. Wollenberger, R. Bernhardt, P. de Oliveira, Direct and mediated electrochemical response of the cytochrome P450 106A2 from Bacillus megaterium ATCC 13368, Bioelectrochemistry 87 (2012) 71-77.
[23] N. Bistolas, U. Wollenberger, C. Jung, F.W. Scheller, Cytochrome P450 biosensors-a review, Biosens. Bioelectron. 20 (2005) 2408-2423.
[24] E.J. Laviron, General expression of the linear potential sweep voltammogram in the case of diffusionless electrochemical systems, Electroanal. Chem. 101 (1979) 19-28.
[25] F.P. Guengerich, Oxidation-reduction properties of rat liver cytochromes P-450 and NADPH-cytochrome p-450 reductase related to catalysis in reconstituted systems, Biochemistry 22 (1983) 2811–2820.
[26] S.G. Sligar, D.L. Cinti, G.G. Gibson, J.B. Schenkman, Spin state control of the hepatic cytochrome P450 redox potential, Biochem. Biophys. Res. Commun. 90 (1979) 925–932.
[27] S. Maurelli, M. Chiesa, E. Giamello, G. Di Nardo, V.E.V. Ferrero, G. Gilardi, S. Van Doorslaer, Direct spectroscopic evidence for binding of anastrozole to the iron heme of human aromatase. Peering into the mechanism of aromatase inhibition, Chem. Commun. (Camb.) 47 (2011) 10737-10739.
[28] W. Jiang, D. Ghosh, Motion and flexibility in human cytochrome p450 aromatase, PLoS One 7 (2012) e32565.
[29] G. Di Nardo, M. Breitner, A. Bandino, D. Ghosh, G.K. Jennings, J.C Hackett, G. Gilardi, Evidence for an elevated aspartate pKa in the active site of human aromatase, J. Biol. Chem. (2014) doi: jbc.M114.595108.
[30] Y.M. Khatri, A. Luthra, R. Duggal, S.G. Sligar, Kinetic solvent isotope effect in steady-state turnover by CYP19A1 suggests involvement of Compound 1 for both hydroxylation and aromatization steps, FEBS Letts. 588 (2014) 3117-3122.

Figure legends.

Scheme 1. The three steps reaction catalysed by aromatase.

Figure 1. A) Square wave, B) original and C) buffer-corrected (thin solid trace) cyclic voltammograms of substrate-free (thick solid line) and AD-bound (dashed line) immobilized rArom. AD concentration was 10 μM, the scan rate for CV was 120 mV sec^{-1}. Inset: plot of cathodic (filled circles) and anodic (open circles) peak currents versus scan rate for substrate-free-rArom on PDDA GC electrodes.

Figure 2. HPLC traces of (A) AD, (B) 19-OHAD obtained from immobilized rArom and incubated with 10 μM of androstenedione, (C) 19-OXOAD obtained starting from 1 μM of androstenedione and (D) estrone obtained from 150 μM of 19-OXOAD. Electrocatalysis experiments (solid black traces) are shown together with control experiments performed in the absence of the protein (solid grey traces) and standards of the compounds (dashed traces).

Table 1. Redox potentials (versus Ag/AgCl) of immobilized aromatase

	E_{red} (mV)	E_{ox} (mV)	E_m (mV)
rArom/PDDA	-285±7	-283±5	-284±8
rArom+AD/PDDA	-248±6	-247±3	-247±3
rArom+19OHAD/PDDA	-248±6	-246±7	-247±6
rArom+19OXOAD/PDDA	-258±2	-256±4	-257±1

Table 2. Summary of the amount of products formed by immobilized rArom electrocatalysis

Starting substrate	Concentration (μM)	19-OHAD (μM)	19-OXOAD (μM)	Estrone (μM)
AD	10	0.15 ± 0.05	Not detectable	Not detectable
AD	1	Below the quantification limits	0.11 ± 0.03	Not detectable
19-OHAD	150	-	0.31 ± 0.01	0.81 ± 0.08
19-OXOAD	150	-	-	1.69 ± 0.17

Scheme 1.

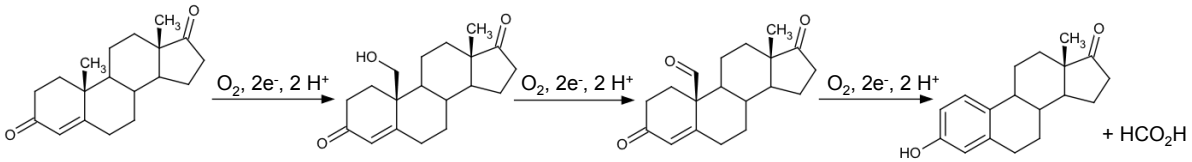

Androstenedione (AD) | 19-hydroxyandrostenedione (19-OHAD) | 19-oxoandrostenedione (19-OXOAD) | Estrone

Figure 1.

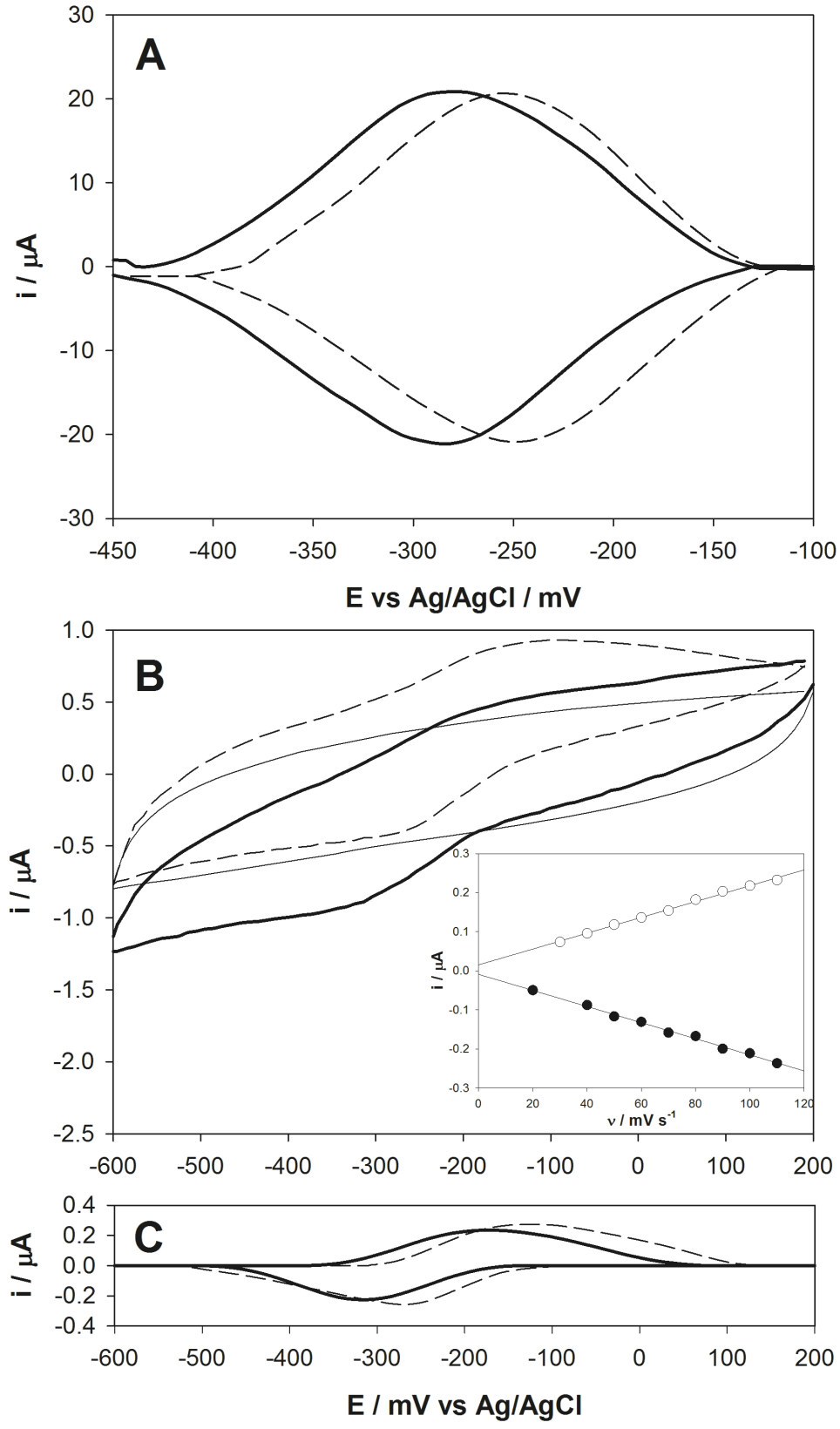

Figure 2.

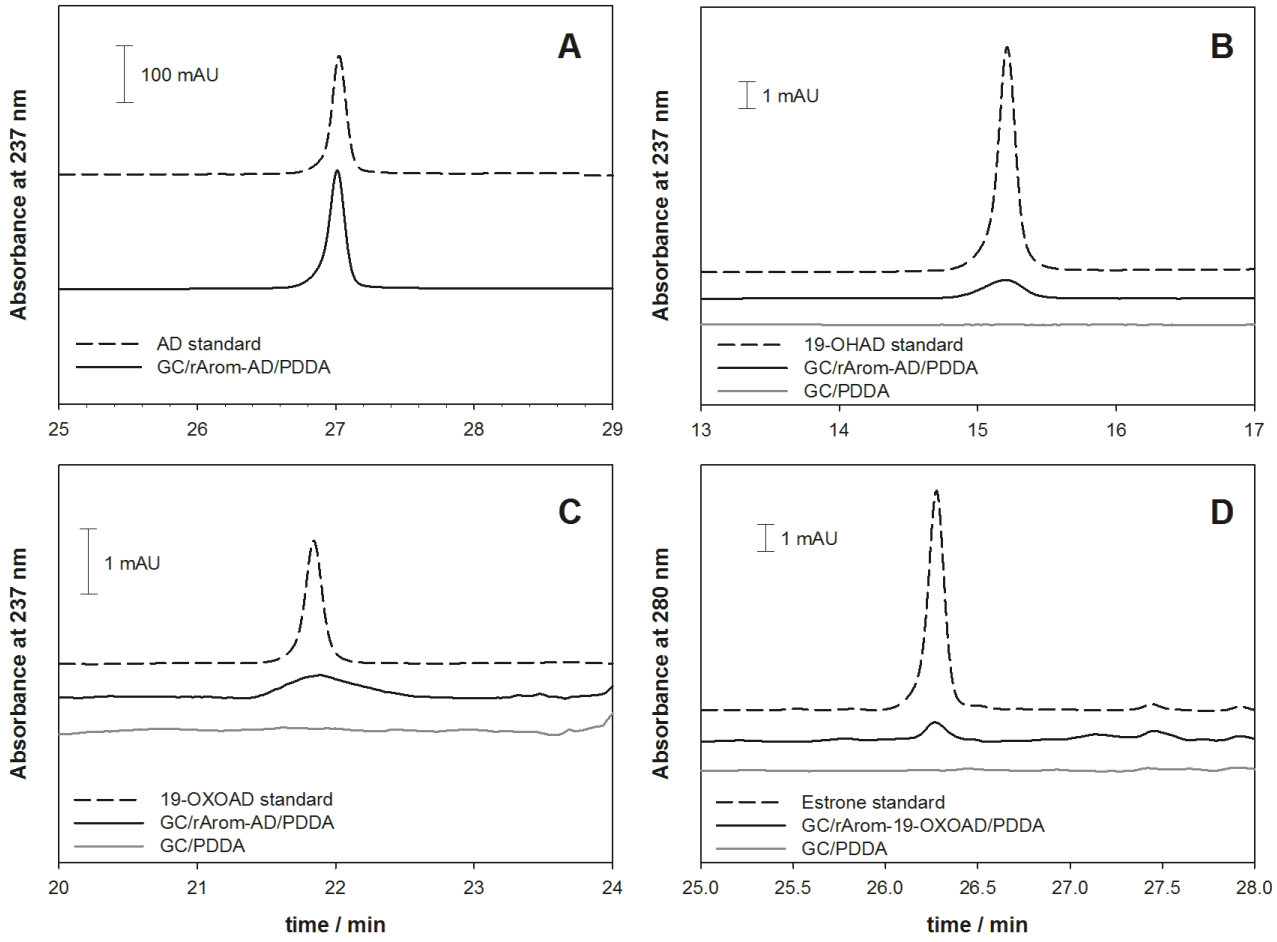
A
100 mAU
Absorbance at 237 nm
AD standard
GC/rArom-AD/PDDA
25
26
27
28
29
B
1 mAU
Absorbance at 237 nm
19-OHAD standard
GC/rArom-AD/PDDA
GC/PDDA
13
14
15
16
17
C
1 mAU
Absorbance at 237 nm
19-OXOAD standard
GC/rArom-AD/PDDA
GC/PDDA
20
21
22
23
24
time / min
D
1 mAU
Absorbance at 280 nm
Estrone standard
GC/rArom-19-OXOAD/PDDA
GC/PDDA
25.0
25.5
26.0
26.5
27.0
27.5
28.0
time / min